J Mater Sci (2008) 43:5516–5520
DOI 10.1007/s10853-008-2821-9

Far infrared properties of PbTe doped with Bismuth

P. M. Nikolic · K. M. Paraskevopoulos · S. S. Vujatovic · A. Bojicic · T. T. Zorba · M. V. Nikolic · B. Stamenovic · T. Ivetic · V. Blagojevic

Received: 20 February 2008 / Accepted: 18 June 2008 / Published online: 18 July 2008

Abstract Far infrared reflectivity spectra of single crystal PbTe doped with Bi were measured and numerically analyzed using a fitting procedure based on a modified plasmon–phonon interaction model with two additional oscillators at about 140 and 219 cm^{-1} which represents local Bi impurity modes. The position of observed plasma minimum and the values of the calculated parameters were compared with the literature data for pure single crystal PbTe which shows that bismuth improved the basic properties of the host crystal a lot.

Introduction

Narrow band-gap IV–VI binary semiconductors and their alloys have been studied a lot because of their fundamental electronic properties and for their practical applications in optoelectronics for making infrared detectors, light-emitting [1, 2] and thermoelectric [3, 4] devices. Lead chalcogenides grow with high deviations from stoichiometry with defects which are electrically active. If we dope these narrow gap semiconductors with some impurities, it results in the appearance of some strong and unusual effects which are not characteristic for undoped samples [1]. If, for instance, PbTe is doped with some group III impurities (B, Ga, and In) that leads to the Fermi level pinning effect. Doping also offers the possibility of varying the lattice parameters, band gap, conductivity type, and carrier concentration. Also, a persistent photoconductivity effect with a long relaxation time was observed at low temperature [5]. When PbTe was doped with group V impurities (As, Sb, and Bi), where the valence configurations are $4p^3$, $5p^3$, and $6p^3$ for As, Sb, and Bi, respectively, deep defect states formed [4] important to attain electron concentrations maximizing the effectiveness of a material for thermoelectric applications. Then the thermoelectric figure of merit ZT becomes optimal. T is the absolute temperature and $Z = (S^2\sigma)/K$ where S is Seebeck coefficient, σ is the electrical conductivity, and K is the thermal conductivity which has two contributions, one from the electrical carriers, K_e, and the other from the thermal lattice vibrations (phonon), $K_{lattice}$. A good thermoelectric material must have both a large power factor ($P = S^2\sigma$) and a low thermal conductivity. Bi is the one of the most important dopants for crystals based on PbTe. When Bi is introduced in p type PbTe, it leads to inversion of the dominant carrier sign from "p" to "n" even for Bi concentrations <0.1 at% [4, 6, 7]. As far as we know nobody has been studied far infrared properties of PbTe doped with Bi, yet. So, in this work we will try to fill that gap.

The nonmonotonic character of the dependences of properties on composition of PbTe + Bi [8] is attributed to the change in the mechanism of Bi dissolution under change in the Bi concentration to self-organization process

P. M. Nikolic (✉) · S. S. Vujatovic · A. Bojicic · B. Stamenovic · T. Ivetic
Institute of Technical Sciences SASA, Knez Mihajlova 35/IV, 11000 Belgrade, Serbia
e-mail: nikolic@sanu.ac.yu

K. M. Paraskevopoulos · T. T. Zorba
Solid State Section, Physics Department, Aristotle University of Thessaloniki, 54124 Thessaloniki, Greece

M. V. Nikolic
Institute for Multidisciplinary Research, Kneza Viseslava 1, 11000 Belgrade, Serbia

V. Blagojevic
Faculty of Electrical Engineering, University of Belgrade, Bulevar kralja Aleksandra 73, 11000 Belgrade, Serbia

in the impurity subsystem of crystal and to percolation effects.

Experimental

Single crystal ingots of PbTe doped with the starting composition of 2 at% Bi were synthesized using the standard Bridgman method [9]. High purity elements (6 N) were used as the source material. The composition of Bi increased along the length of the ingot, and a number of samples with different Bi content were cut and polished. The samples were examined with X-ray and it was confirmed that they were single crystals which could be cleaved perpendicular to the *c*-axis. No signs of nanocrystalization states were noticed. Highly polished samples were used for optical reflectivity measurements which were done using a Bruker IFS-113 V Fourier transform spectrometer whose resolution was about 1 cm^{-1}. For the measurements, we used a polarizer to see if our single crystal sample is sensitive to light polarization.

Results and discussion

The room temperature reflectivity diagram, as a function of the wave number, for a single crystal PbTe sample doped with 0.2 at% Bi (S_1) is given in Fig. 1.

In this case, the polarized light was parallel to *c*-axis. For the light beam polarized perpendicular to the *c*-axis of the same sample, the measured reflectivity spectrum is given in Fig. 2 (S_2).

It is interesting to notice that these two diagrams are a bit different when the light beam was differently polarized. For both diagrams, the plasma minimum is rather sharp and at an unusually low frequency. That is characteristic of PbTe samples with a low free carrier concentration and high mobility [10]. For both diagrams, S_1 and S_2, one can see a maximum at about 140 cm^{-1} which could be regarded as a local mode of dopant Bi. But for normal polarization to the *c*-axis (Fig. 2), there is another less exposed maximum at about 219 cm^{-1} which should be carefully analyzed because it might belong to another Bi mode.

Far infrared reflectivity spectrum of single crystal sample PbTe doped with 0.4 at% Bi is shown in Fig. 3. Finally, reflectivity spectrum from a sample cut from the same ingot near its end, which was doped with 2 at% Bi, is given in Fig. 4. One can notice that the plasma minimum moves toward the higher frequencies when the content of Bi was increased. It is at about 120 cm^{-1} when PbTe was doped with 0.2 at% of Bi (Fig. 1) and then at about 160 cm^{-1} for 0.4 at% Bi (Fig. 3) and then changed a lot

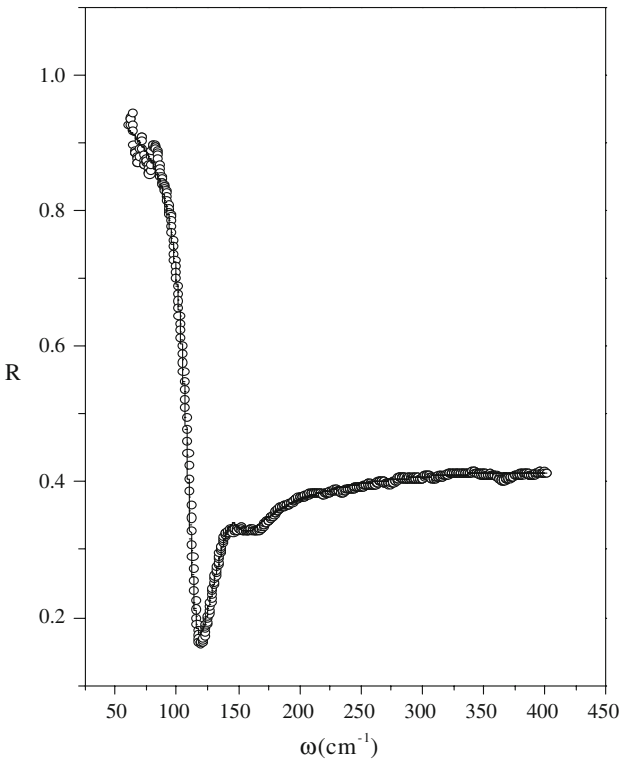

Fig. 1 Room temperature reflectivity diagram of PbTe with 0.2 at% Bi with polarized light parallel to the *c*-axis. Experimental results are given with circles, while the full line was calculated using a fitting procedure based on the model given by Eq. 1

when PbTe was doped with 2 at% Bi to about 500 cm^{-1} (Fig. 4).

Reflectivity spectra could be interpreted with the help of a frequency dependant dielectric function. We used a four parameter model [11] where a combined plasmon–LO phonon mode was present [12]. Then the determination of the LO mode is connected with the elimination of the free carrier influence. Finally, the dielectric function takes into account the presence of a plasmon LO phonon interaction:

$$\varepsilon(\omega) = \varepsilon_\infty \frac{\prod_{j=1}^{2}(\omega^2 + i\gamma_{1j}\omega - \omega_{1j}^2)}{\omega(\omega + i\gamma_p)(\omega^2 + i\gamma_t\omega - \omega_t^2)} \times \prod_{n=1}^{r} \frac{(\omega^2 + i\gamma_{L_n}^2\omega - \omega_{L_n}^2)}{(\omega^2 + i\gamma_{0_n}\omega - \omega_{0_n}^2)} \prod_{k=1}^{q} \frac{(\omega^2 + i\gamma_{LOk}\omega - \omega_{LOk}^2)}{(\omega^2 + i\gamma_{TOk}\omega - \omega_{TOk}^2)} \quad (1)$$

where ω^{ij} and γ_{ij} are parameters of the first numerator representing the eigenfrequencies and damping factor of the plasmon–LO phonon waves, respectively.

Similarly, the first denominator parameters correspond to transverse (TO) vibrations. ε_∞ represents the high frequency dielectric permittivity relative to the interval of measurements and γ_p is the plasmon mode damping factor. The second term in Eq. 1 represents Bi-impurity local modes where ω_{01} and ω_{02} are characteristic impurity mode

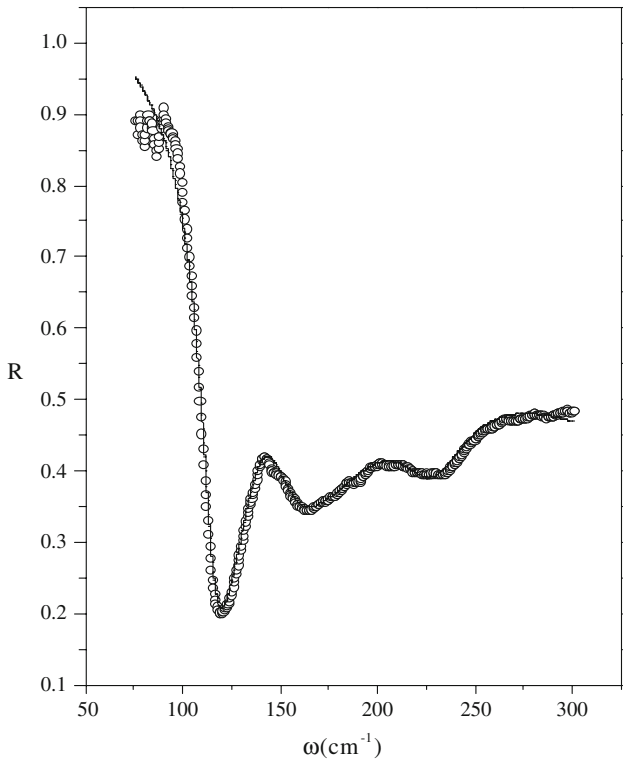

Fig. 2 Room temperature reflectivity diagram with light beam polarized perpendicular to the *c*-axis. Experimental results are given with *circles*, while the *full line* was calculated using a fitting procedure

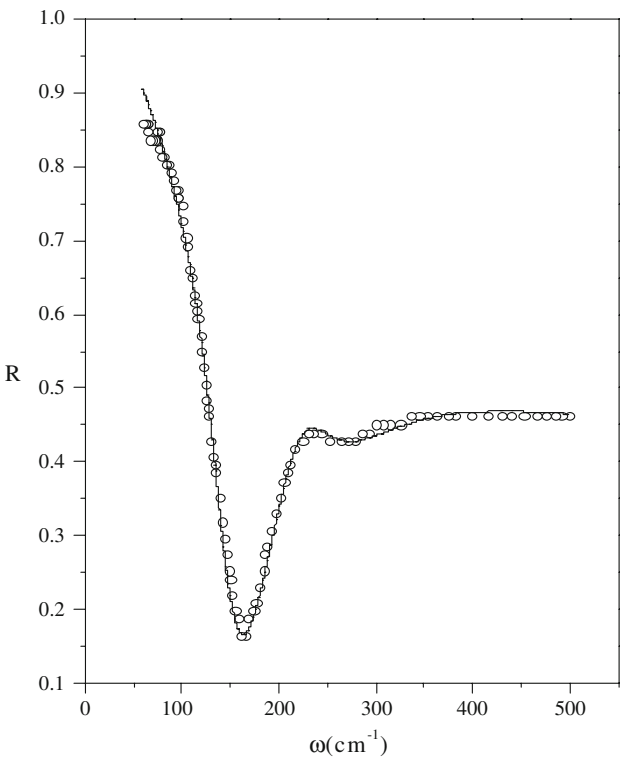

Fig. 3 Far infrared reflectivity spectrum of single crystal sample PbTe doped with 0.4 at% Bi. Experimental spectrum is presented by circles. The *solid line* is calculated spectrum obtained by a fitting procedure

frequencies. Frequencies ω_{L1} and ω_{L2} are parameters connected with the oscillator strength (S) and γ_{01}, γ_{02}, γ_{L1}, and γ_{L2} are their damping factors, respectively. Uncoupled modes of PbTe are ω_{LOk}, ω_{TOk} (longitudinal and transverse frequencies) and γ_{LOk}, γ_{TOk} their damping factors.

The values of plasma frequency, ω_p, were determined using the following equation:

$$\omega_p = \frac{\omega_{11} \cdot \omega_{12}}{\omega_t} \tag{2}$$

where ω_t, the transverse phonon frequency for PbTe was taken from literature [13] to be 32 cm^{-1} because our reflectivity spectra we measured only down to 50 cm^{-1}.

For fitting procedure, the starting values of all parameters were previously determined using Kramers Krönig analysis.

The values of the parameters calculated using Eqs. 1 and 2 are given for all samples in Table 1. The values of their error bars are smaller than 1 cm^{-1}. Optical mobility of free carriers was calculated using the method of Moss et al. [14].

Looking at Table 1, one can see that first two plasma frequencies are slightly different and at a rather low frequency. For sample S_1, the plasma damping factor is also a bit smaller and the optical mobility of free carriers is about

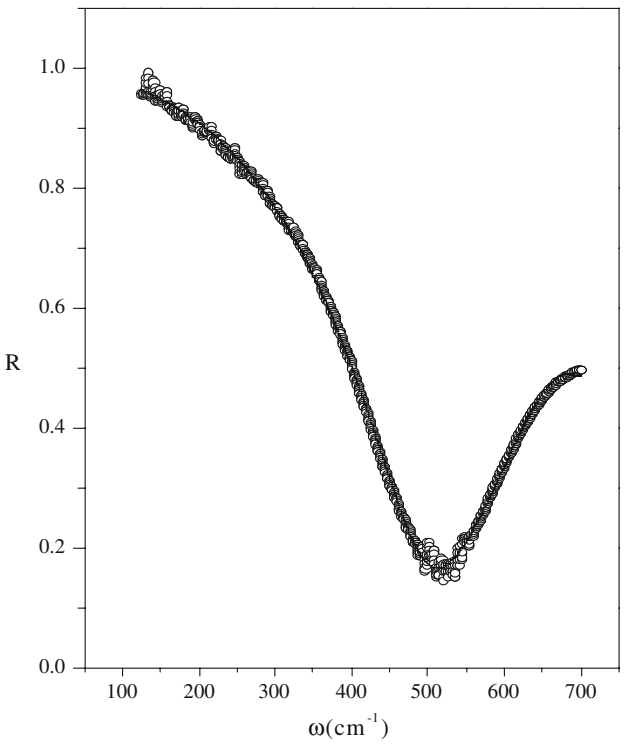

Fig. 4 Far infrared reflectivity spectrum of single crystal sample PbTe doped with 2 at% Bi. The *solid line* is calculated spectrum obtained by a fitting procedure

Table 1 Optical parameters determined for PbTe doped with Bi

%Bi	ω_{11}	γ_{11}	ω_{12}	γ_{12}	ω_{01}	γ_{01}	ω_{L1}	γ_{L1}	ω_{01}	γ_{02}	ω_{L2}	γ_{L2}	ω_p	μ_n
S_1 (0.2 at%)‖c	113.5	12.7	30	11.4	144.7	2.4	148	29	219	769	237	779	106	4648
S_2 (0.2 at%)⊥c	115.7	14.4	30	35	140	21.5	152.6	39	219	70	227	36	108	3800
S_3 (0.4 at%)	160	41.7	30	41.7	144	21	148	29	226	52.7	240	118.6	150.4	2684
S_4 (2 at%)	499.6	149	30	128	144.7	1095	579	307	230	832	244	838	468.4	285

All values are given in cm^{-1}, except μ_n which is given in $cm^2\ V^{-1}\ s^{-1}$

22% higher than for S_2. In both cases, the optical mobility is very high compared with the literature value for n-type PbTe which is only 1730 cm^2/V s.

The sample with 0.4 at% Bi (S_3) also has a higher electron optical mobility compared with pure n-type PbTe. Here it should be emphasized that the optical mobility for the sample with 2 at% Bi decreased to only 285 cm^2/V s. Recently, Rogacheva et al. [15] reported electron mobility of PbTe crystals doped with Bi whose concentration was between 0.1 and 1 at% Bi of about 4000 cm^2/V s at 80 K and at room temperature of about 600 cm^2/V s. Our single crystal sample of PbTe doped with 0.2 at% has higher room temperature optical electron mobility of about 4600 cm^2/V s when the light was polarized parallel to the *c*-axis and a slightly lower value of 3800 cm^2/V s for the light polarized normal to the *c*-axis. When the content of Bi was increased to 0.4 at% or even 2 at% then the mobility decreased to 2800 cm^2/V s and finally to only 285 cm^2/V s. This increase of optical electron mobility with decrease of content of Bi was followed by decrease of the plasma frequency with a minimum at about 106 cm^{-1}.

Obviously those lower concentrations of Bi (0.2 at%) resulted in better properties of the crystal. Similarly in the literature, the optimal concentration of Ga in PbSnTe was 0.2 at% [16] and for PbTe doped with Cr [17]. This means that low concentrations of Bi atoms are located on the Pb cation sites and the system is an n-type semiconductor and electrons in PbTe move in predominantly Pb-based orbitals. When the Bi concentration is increased a lot—above 0.4 at% Bi then one can expect some Bi atoms to enter into interstitial positions. Then, the space distribution of the impurity could probably be observed by atomic and electron microscopy.

Now the question could arise how many local modes could PbTe doped with Bi have. We actually observed two local modes, one at about 140 cm^{-1} and another at 219 cm^{-1}. Bi behaves similarly to Ga and Tl, which belong to the type of trivalent impurity, group III. The valence configurations of the group III trivalent atoms are $4s^24p^1$, $5s^25p^1$, and $6s^26p^1$ for Ga, In, and Tl, respectively. The valence configurations of the group V trivalent atoms are $4p^3$, $5p^3$, and $6p^3$ for As, Sb, and Bi, respectively. The calculation of the electronic density states for PbTe doped with either group III or group V trivalent atoms show that for In the deep defect state lies in the band gap region, while for the Ga atom the deep defect state is near the top of the PbTe valence band [18]. In contrast to group III impurities the resonant states of Bi, with *p* valence electron impurities, are near the bottom of the conduction band. Similarly to PbTe doped with Ga, In, or Tl, one can suppose that, when PbTe is doped with Bi, there is an unstable Bi^{2+} state which may transfer to a less unstable form: $2Bi^{2+} = Bi^{1+} + Bi^{3+}$. Also the Bi^{1+} state can transfer as follows: $Bi^{1+} = Bi^{3+} - 2e$. The metastable state (Bi^{2+}) for single crystal PbTe doped with Bi, we believe is at about 140 cm^{-1} while another stable state at 219 cm^{-1} belongs to Bi^{1+}. Finally the Bi^{3+}, empty center, which we did not observe might be at a higher frequency. It is interesting to mention that Ahmad et al. [18] for PbTe doped with In did not find any evidence for the presence of an In^{3+} state either. Following the behavior of the local phonon modes of impurities, the principal properties of the PbTe matrices doped by different cations are determined by anharmonic electron–phonon interactions as shown during an investigation of nonlinear optical properties of these materials [19].

Conclusion

In this work far infrared reflectivity spectra of PbTe doped with 0.2, 0.4, and 2 at% Bi were measured with polarized light at room temperature and numerically analyzed. Beside the strong plasma–LO phonon interaction two impurity local modes at 140 and 219 cm^{-1}, which correspond to the impurity atom in different valence states, were observed and numerically analyzed. The lower frequency mode can be assumed to be a local bismuth mode representing the population of a metastable state Bi^{2+}. The other local mode at about 219 cm^{-1} could be the result of electron transfer from the stable two electron state to the conduction band. The calculated optical mobility of free carriers for the PbTe sample doped with 0.2 and 0.4 at% Bi was much higher compared to single crystal pure PbTe. This means that PbTe doped with a small percentage of Bi will achieve higher thermoelectric properties due to the coexistence of high free carrier mobility. This is important because PbTe is one of the best thermoelectric materials

used for thermoelectric generators in the temperature range between 400 and 800 K [20].

References

1. Akimov BA, Dimitriev AV, Khokhlov DR, Ryabova LI (1993) Phys Status Solidi A 137:9. doi:10.1002/pssa.2211370102
2. Schiessl UP, John J, McCann PJ (2004) In: Choi HK (ed) Long wavelength infrared semiconductor laser. Wiley and Sons, Hoboken, NJ
3. Rowe DM (1995) CRC handbook of thermoelectrics. CRC Press, London
4. Dresselhous MS, Lin MY, Koga T, Cronin SB, Rabin O, Black MR, Dresselhous G (2001) In: Tritt TM (ed) Semiconductors and semimetals: recent trends in thermoelectric materials research III. Academic Press, Burlington, MA
5. Romcevic N, Popovic ZV, Khoklov DR, König W (1997) Infrared Phys Technol 38:117. doi:10.1016/S1350-4495(96)00042-4
6. Tavrina TV, Rogacheva EI, Pinegin VI (2005) Mold J Phys Sci V4(4):430
7. Rogacheva EI, Lyubchenko SG (2005) Thermoelectricity 3:23
8. Rogacheva EI, Lyubchenko SG, Vodarez OS, Kuzmenko AM, Dresselhous MS (2006) In: Proceedings of 17th inter. conference on thermoelectronics, p 656
9. Akimov BA, Ryabova LI, Yatsenko OB, Chudinov SM (1989) Tekh Poluprovodn 23:1019
10. Nikolic PM, Lukovic D, König W, Nikolic MV, Blagojevic V, Vujatovic SS, Savic S, Stamenovic B (2008) J Optoelectr Adv Mater 10:145
11. Gervais F, Piriou B (1974) Phys Rev B 10:1642. doi:10.1103/PhysRevB.10.1642
12. Kukharski AA (1970) Solid State Commun 8:1275. doi:10.1016/0038-1098(70)90619-8
13. Romcevic N, Popovic ZV, Khokhlov DR, König W (1997) Infrared Phys Techn 38:117. doi:10.1016/S1350-4495(96)00042-4
14. Moss TS, Hawkins TD, Burrell GJ (1968) J Phys 1:1435
15. Rogacheva EI, Lyubchenko SG, Vodorez OS (2006) Funct Mater 13:571
16. Skipetrov EP, Zvereva EA, Dmitriev NN, Golubov AV, Slyn'ko VE (2006) Semiconductors 40:893. doi:10.1134/S1063782606080069
17. Akimov BA, Vertelecki PV, Zlomanov VP, Ryabova LI, Tananaeva OI, Sirokova NA (1989) Phys Techn Semicond 23:244
18. Ahmad S, Mahanti SD, Hoang K, Kanatzidis MG (2006) Phys Rev B 74:155205. doi:10.1103/PhysRevB.74.155205
19. Nouneh K, Kityk IV, Viennois R, Benet S, Charar S, Paschen S et al (2006) Phys Rev B 73:035329-1. doi:10.1103/PhysRevB.73.035329
20. Vining Cronin B (2007) In: Proceedings of the European conference on thermoelectronics, EC 1200/Odessa